The Journal of Experimental Biology 200, 55–64 (1997)
Printed in Great Britain © The Company of Biologists Limited 1997
JEB0445

MITOCHONDRIA-RICH CELLS IN GILLS OF TILAPIA (*OREOCHROMIS MOSSAMBICUS*) ADAPTED TO FRESH WATER OR SEA WATER: QUANTIFICATION BY CONFOCAL LASER SCANNING MICROSCOPY

A. J. H. VAN DER HEIJDEN*, P. M. VERBOST, J. EYGENSTEYN, J. LI, S. E. WENDELAAR BONGA AND G. FLIK

Department of Animal Physiology, Faculty of Science, University of Nijmegen, Toernooiveld, 6525 ED Nijmegen, The Netherlands

Accepted 11 September 1996

Summary

We used confocal laser scanning microscopy to validate a new and fast co-labelling method to study the distribution of mitochondria-rich (MR) cells in gill filaments and to differentiate between MR cells that are in contact with the water (cells labelled with both DASPMI and Concanavalin-A) and those that are not (DASPMI-positive only). This method was used to describe differences in MR cell density that occur in the gills of tilapia *Oreochromis mossambicus* adapted to fresh water or sea water. In fresh water, the total MR cell density was 6233 cells mm^{-2} and the density of the subpopulation of MR cells that are in contact with the water was 3458 mm^{-2}. After seawater adaptation, cell density decreased to 3061 cells mm^{-2} for all MR cells of which 2445 cells mm^{-2} were in contact with water. The percentage of double-labelled MR cells in the total MR cell population had increased from 55 to 80 %. MR cell size (measured as the maximal cross-sectional area) increased from 87 μm^2 in fresh water to 217 μm^2 in sea water.

Biochemical determination of specific and total Na^+/K^+-ATPase activity in gill homogenates showed no difference between freshwater- and seawater-adapted fish. Quantification of 'mature' chloride cell density in fixed gill filaments using scanning electron microscopy resulted in an overestimate of chloride cell density due to shrinkage of the sample.

Key words: tilapia, *Oreochromis mossambicus*, gills, fresh water, sea water, chloride cells, DASPMI, Concanavalin-A, quantification, confocal laser scanning microscopy, electron microscopy, Na^+/K^+-ATPase.

Introduction

The branchial epithelium serves a primary role in the osmoregulation of fish, and many studies have attempted to relate changes in branchial ion turnover to changes in the ultrastructure and/or changes in the turnover and biochemical capacities of the ion-transporting cells of the epithelium, the chloride cells (de Renzis and Bornancin, 1984; Hwang, 1987; Pisam and Rambourg, 1991; Flik and Verbost, 1993). Chloride cells have all the characteristic features of ion-transporting cells (Berridge and Oschman, 1972): an abundance of mitochondria, an extended tubular system where ion-transporting enzymes such as Na^+/K^+-ATPase, Ca^{2+}-ATPase and Na^+/Ca^{2+} exchangers are located (Karnaky *et al.* 1976; Flik *et al.* 1985*a*; Perry and Flik, 1988; Verbost *et al.* 1994) and contact with both blood and water. We will illustrate the ion-transport activities of the chloride cells using two examples, Ca^{2+} and Cl^- transport.

Many studies on chloride cell function use the opercular membrane, which acts as a model for the gills and may be mounted in an Ussing chamber. A positive correlation has been found between chloride cell density and Ca^{2+} influx in the opercular membrane of a variety of fish (McCormick *et al.* 1992; Marshall *et al.* 1995), the flux extrapolated to a 'zero' chloride cell density being negligible. From this type of study, it has been suggested that the chloride cell plays a pivotal role in Ca^{2+} uptake. In a study comparing freshwater- and seawater-adapted tilapia *Oreochromis mossambicus* (Flik *et al.* 1996), the branchial influx of Ca^{2+} was very similar, irrespective of the external medium, suggesting that chloride cells have similar Ca^{2+} transport mechanisms in fresh water and in sea water (Verbost *et al.* 1994). However, when the branchial transport of Cl^- is studied, a different picture emerges. Cl^- is transported across the plasma membranes of the chloride cells for housekeeping purposes (in particular for volume regulation) and for osmoregulation (net ion transport). In fresh water, Cl^- is taken up from the water through the action of a 4-acetamido-4′-isothiocyanostilbene-2,2′-disulfonic acid- (SITS-) sensitive Cl^-/HCO_3^- exchanger (Perry and Randall, 1981) and is assumed to move to the blood compartment *via* Cl^- channels in

*e-mail: angeliq@sci.kun.nl.

the basolateral plasma membrane. In sea water, where the fish drinks a high-[Cl^-] solution (Smith, 1930), the surplus Cl^- absorbed through the intestine is excreted through the gills. The amount of Cl^- transported through the chloride cells increases significantly and the direction of the transport is reversed. A bumetanide-sensitive Cl^- transporter may fulfil an important role in the transport of Cl^- across the basolateral plasma membrane, both in volume regulation and in secretion (Zadunaisky *et al.* 1995). It follows that chloride cells in fish in sea water must differ from those in fresh water, and adaptation to these media requires either replacement of cells or changes in the membrane composition of existing cells.

Insight into the function of chloride cells would be obtained if the occurence of different (accessory, immature, mature and apoptotic) stages of the chloride cell cycle could be quantified. Only 'mature' cells, which contact the water (*via* the apical pit) and blood (*via* the basolateral membrane), are thought to be involved in ion transport (Wendelaar Bonga and van der Meij, 1989; Wendelaar Bonga *et al.* 1990). Conventional methods for the quantification of chloride cells all have drawbacks. First, identification of chloride cell populations using fluorescent probes for mitochondria (Karnaky *et al.* 1984; Wendelaar Bonga *et al.* 1990; Kültz *et al.* 1992) or biochemical methods (Flik *et al.* 1995) does not distinguish between the developmental stages. Second, scanning electron microscopy (SEM) only allows identification of the apical surface of mature cells (Perry *et al.* 1992). Third, transmission electron microscopy (TEM) enables the detection of accessory, immature, mature and degenerating (apoptotic and necrotic) chloride cells (Wendelaar Bonga *et al.* 1990; Pratap and Wendelaar Bonga, 1993), but is, in our view, too laborious to be used for routine analysis.

We have used confocal laser scanning microscopy (CLSM) to validate a new and fast co-labelling method (Li *et al.* 1995) enabling us to differentiate between mitochondria-rich (MR) cells that are in contact with the water and those that are not. We have used this method to describe the differences in MR cell density that occur in gills of the euryhaline tilapia *Oreochromis mossambicus* when it is adapted to either fresh water or sea water. We have compared our results with data obtained using the more conventional techniques of biochemically determining Na^+/K^+-ATPase activity in gill homogenates and examining gill filaments using electron microscopy (TEM and SEM).

The fluorescent double-labelling technique provides a fast and valuable method for qualitatively and quantitatively assessing MR cells in gill filaments and it forms a powerful tool in the study of the function of these cells. An important finding of this study was that in fixed gill epithelium the absolute numbers for chloride cell density are overestimated owing to shrinkage of the sample.

Materials and methods

Fish maintenance and holding conditions

Freshwater Mozambique tilapia (*Oreochromis mossambicus* Peters), body mass 15–65 g) obtained from laboratory stock, were kept in city of Nijmegen tap water ($[Na^+]$=0.9 mmol l^{-1}, $[Cl^-]$=1.0 mmol l^{-1}, $[Ca^{2+}]$=0.8 mmol l^{-1}). Artificial sea water (density 1.022 g l^{-1}) was prepared by dissolving natural sea salt (Wimex, Krefeld, Germany) in tap water. Fish were first transferred to half-strength sea water and then, after 1 day, to full-strength sea water ($[Na^+]$=502 mmol l^{-1}, $[Cl^-]$=621 mmol l^{-1}, $[Ca^{2+}]$=10.1 mmol l^{-1}). They were kept in sea water for 4 weeks before experimentation. The water temperature was 25 °C and the photoperiod was 12 h. Food was supplied at a daily ration of 1.5 % of the total body mass.

Confocal laser scanning microscopy

Fish were killed by spinal transection. The second gill arch was dissected and transferred to a tilapia Ringer, containing (in mmol l^{-1}): 146 NaCl, 3 KCl, 1 $CaCl_2.7H_2O$, 1 $MgSO_4.7H_2O$, 1 NaH_2PO_4, 15 $NaHCO_3$, 5 Tris and 10 glucose (pH 7.4). Individual filaments were carefully separated and incubated with fluorescent dyes dissolved in this Ringer. The filaments were first incubated for 30 min with Concanavalin-A (Con-A), a lectin from jack bean *Canavalia ensiformis*, coupled to fluorescein (15 μg ml^{-1} Con-A–fluorescein conjugate in tilapia Ringer; Molecular Probes; excitation 495 nm, emission 520 nm). This lectin was found empirically to bind strongly to the apical membrane (or 'pit') of MR cells (Li *et al.* 1995). After rinsing, the filaments were incubated in tilapia Ringer containing 6–12 μl ml^{-1} of a saturated dimethylaminosteryl-methylpyridiumiodine (DASPMI, Molecular Probes, excitation 472 nm, emission 609 nm) solution in water for 10–20 min to label mitochondria-rich (MR) cells (Bereiter-Hahn, 1976; Karnaky *et al.* 1984). After a final wash, the labelled filaments were placed on glass slides (with the lamellae orientated perpendicular to the glass support) in a drop of tilapia Ringer, surrounded by silicone grease. A coverslip was placed gently on top to prevent fluid evaporation.

A confocal laser scanning microscope (Biorad MRC-600), equipped with an argon laser and a Nikon Optiphot microscope (40×, 1.3 NA oil-immersion objective), was used in combination with excitation by blue light (488 nm), a 515 nm emission barrier filter set (BHS) and an A2 filter (blocking emission wavelengths below 600 nm). With this set-up, the emission wavelengths of DASPMI and Con-A–fluorescein conjugate are separated and transmitted to different photomultipliers. The pictures from each photomultiplier were subsequently merged in false colour to visualize the labels simultaneously.

For quantification of the density of MR cells and apical crypts, consecutive optical sections ('*z*-scans', 0.5 μm thick, 1 μm apart) were made in a plane parallel to the mucosal surface of the filament and to a depth of one cell layer (approximately 12 μm in fresh water and 20 μm in sea water). Merged *z*-scans made it possible to discriminate between MR cells that were in contact with the water (double-labelled) and those that were not (DASPMI-positive only). Cells or particles that were Con-A-positive only were seldom seen and were not included in cell counts. Using this technique, the total number

of MR cells and pits could be counted, as well as the number of individual MR cells with a pit, since pits were sometimes shared by two or more cells. Measurements were restricted to the top MR cell layer beneath the pavement cell layer, in a mid-region of the filament. In this area, a flat section (measuring 2500 μm^2) was chosen behind the secondary lamellae on the trailing edge (where the afferent arteries are situated, see also Fig. 1). At least four fish per group and three filaments per fish were scanned. Three observations were made on each filament. CLSM sampling time was approximately 5 min.

For determination of MR cell size, cells with visible nuclei were randomly selected (10 per fish; 40 cells per group) and cell area was measured (MRC-600 SOM software). Calibration was achieved using a standard calibrated slide.

Transmission electron microscopy

Gill filaments of freshwater-adapted fish were labelled with Concanavalin-A to determine the cell type(s) to which this lectin binds. Individual filaments were fixed immediately after excision using 3 % glutaraldehyde buffered with phosphate-buffered saline (PBS) for 15 min. They were then incubated in PBS containing 0.4 mg ml^{-1} biotinylated Concanavalin-A (Pierce) for 1 h. After several rinses with PBS, the filaments were incubated for 2 h with PBS containing a 1:25 dilution of a streptavidin albumin-gold (10 nm) solution (Sigma). Controls were treated similarly, except that no biotinylated Concanavalin-A was present during the incubation. Post-fixation was carried out using 3 % glutaraldehyde in PBS for 15 min and a similarly buffered mixture (1:2:1) of 3 % glutaraldehyde, 2 % osmium tetroxide and distilled water for 1 h on ice. Subsequently, the fixed filaments were dehydrated in graded ethanols and embedded in Spurr's resin. Unstained sections were examined using a Philips 201 electron microscope.

Scanning electron microscopy

Immediately after excision, individual filaments from the second gill arches were prefixed in 3 % (v/v) glutaraldehyde in cacodylate buffer (0.1 mol l^{-1}, pH 7.4) for 15 min and subsequently fixed in a mixture (1:1:1) of 3 % glutaraldehyde, 2 % osmium tetroxide and 5 % potassium dichromate for 1 h on ice, washed with several changes of distilled water and then dehydrated in graded ethanols. The tissue was critical-point-dried using liquid CO_2, mounted on a sample holder, covered with gold and then viewed using a Jeol JSM-T300 scanning microscope. Ten different filaments per fish and three fish per group were analyzed from the same area as used for CLSM analysis (Fig. 1). Photographs of this area were used to determine the number and size of the pores in the epithelial surface over an area of 2200 μm^2 (Kontron MOP image analyzer). Calibration was achieved using a standard calibration specimen (2160 lines mm^{-1}).

Comparison between fresh and fixed tissue

To investigate the effect of fixation on the filament, five individual filaments from freshwater-adapted fish were photographed using phase contrast (10× objective) and subsequently fixed for SEM. The length between 10 lamellae and the width of the mid-region of the same filament were measured before and after fixation. In order to determine the effect of fixation at the cellular level, the surface area of pavement cells (a cell type that can be visualized both by CLSM and SEM) was measured. Preparation of the filaments was as described for CLSM and SEM. For CLSM, the surface of pavement cells with its characteristic microridges was labelled with Concanavalin-A–fluorescein conjugate (which binds to the glycocalyx) and visualized using a 60× oil-immersion objective.

Na^+/K^+-ATPase activity in gill homogenates

Na^+/K^+-ATPase activity in gill cell homogenates was determined as described previously (Flik *et al.* 1983, 1985*b*). Na^+/K^+-ATPase activity was defined as Na^+- and K^+-dependent, ouabain-sensitive adenosine triphosphatase activity.

Statistics

Statistical significance of differences between mean values was tested using the Student's or Welch's *t*-test for unpaired data, where appropriate, with $P<0.05$ as the fiducial limit. Significant differences between freshwater and seawater groups are indicated using asterisks.

Results

Confocal laser scanning microscopy

Fig. 2 shows CLSM scans of the double-labelled, non-fixed gill epithelium of freshwater- and seawater-adapted tilapia. Although the filament is a multilayered epithelium consisting of many different cell types (pavement cells, mucous cells, chloride cells etc.), the use of the specific fluorescent labels in combination with CLSM allows visualization of the MR cells and their apical surfaces only. In both freshwater- and seawater-adapted fish, DASPMI-positive (MR) cells are found on the trailing edge and the interlamellar regions of the primary filament epithelium (Fig. 2A). The filament epithelium consists of multiple layers of DASPMI-positive cells (data not shown). Intense staining with fluorescein-conjugated Concanavalin-A, associated with globular-to-cylindrical structures, was restricted to the apical region of the top layer of cells of the epithelium. We will refer to these structures as 'pits'. Fig. 2E shows a reconstructed side-view of a double-labelled epithelium. This picture, which is composed of 33 optical sections in the *z*-direction, clearly shows that both labels are confined to the same cell. The specificity of lectin labelling in apical crypts of MR cells was confirmed using transmission electron microscopy (Fig. 3).

In seawater-adapted tilapia, the size of the (DASPMI-positive) MR cells had more than doubled compared with that in freshwater-adapted fish (Table 1). As a consequence, the total MR cell density in the surface layer was approximately

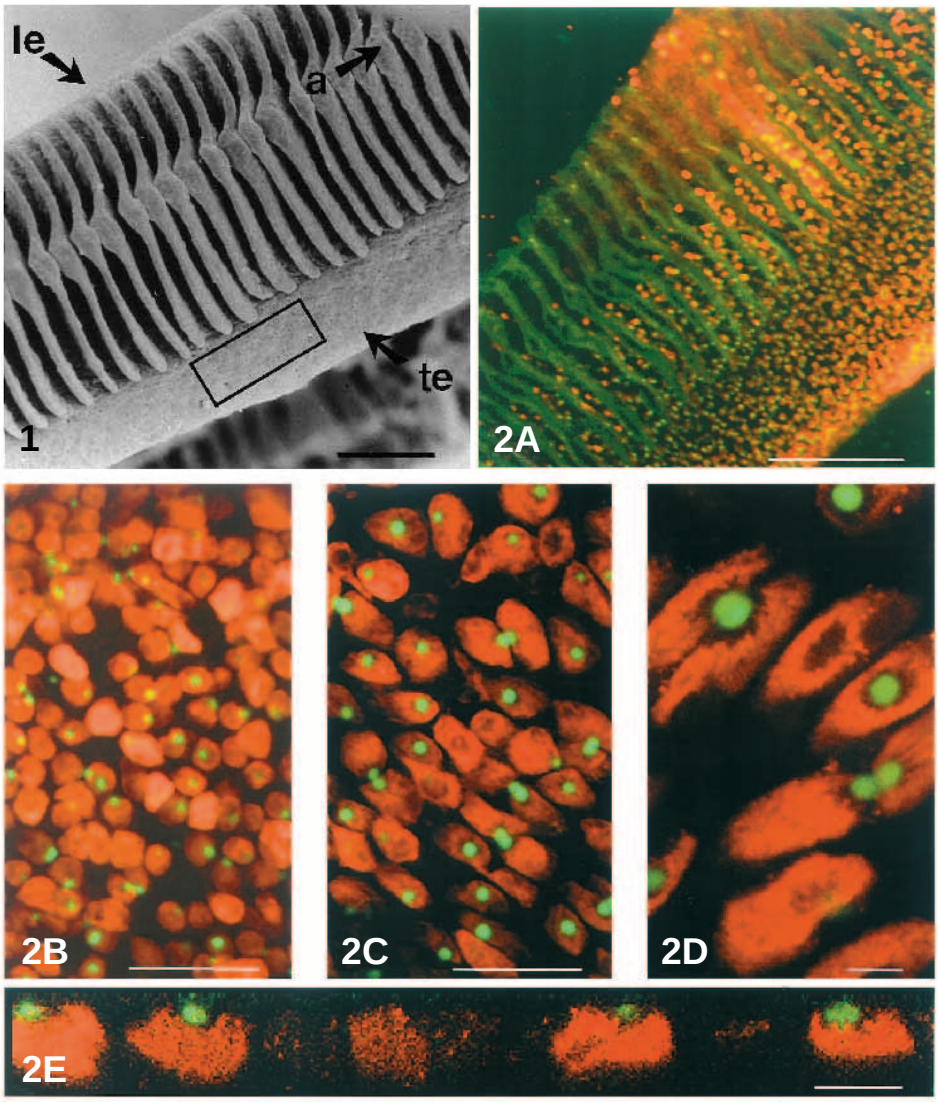

Fig. 1. Scanning electron micrograph of tilapia gill filament indicating the area (rectangle) analysed using different microscopical techniques. le, leading edge; te, trailing edge; the arrow marked 'a' points to the gill arch, to which the filament is connected. Scale bar, 100 µm.

Fig. 2. Confocal laser scanning micrograph of the non-fixed gill filaments (taken from the area indicated in Fig. 1) of freshwater- (A and B) or seawater- (C, D and E) adapted tilapia after co-labelling with Concanavalin-A–fluorescein conjugate (green) and DASPMI (red). (A) Optical section of the middle part of a filament. Co-labelled cells are found on the trailing edge and the interlamellar spaces of the primary epithelium. Note the contours (green) of the secondary lamellae. Scale bar, 250 µm. (B) Superimposed picture of optical sections (0.5 µm thick, 1 µm apart) of the filament near the base of the secondary lamellae showing both stains simultaneously. Scale bar, 50 µm. (C) As in B but from seawater-adapted tilapia. Note that the DASPMI-positive cells are larger than in freshwater fish. Scale bar, 50 µm. (D) Optical section showing multicellular complexes with two DASPMI-positive cells sharing a crypt. Scale bar, 10 µm. (E) Side-view of 33 superimposed optical sections (0.5 µm thick, 1 µm apart) showing four co-labelled cells on the gill filament. DASPMI (red) labels the cytosol and Concanavalin-A–fluorescein conjugate (green) binds to the apical surface of the cell. Scale bar, 10 µm. The less clear DASPMI-labelled cells represent cells that were only partly or sagittally sectioned.

50 % of that in freshwater gills. In addition, the absolute number of pits per mm^2 and the absolute number of MR cells containing a pit (mature MR cells) decreased after seawater adaptation. However, the relative frequency of MR cells featuring a pit increased from 55 % to 80 %.

In both freshwater- and seawater-adapted fish, formation of multicellular complexes with two or more DASPMI-positive cells sharing one pit (Fig. 2D) occurred, but their frequency increased more than 10-fold after seawater adaptation (from 1.1 % to 12.8 %).

Scanning electron microscopy

Fig. 4A shows a scanning electron micrograph of the surface of the primary filament (selected area as in Fig. 1) of a freshwater-adapted tilapia. The surface of the gill is covered with pavement cells, which exhibit microridges arranged in concentric patterns. Three types of pits were distinguished in the epithelium. The first two types had a flat or slightly invaginated surface (Table 2; Fig. 4A). These pits were filled either with very small cellular extensions, which gave them a honeycomb-like appearance (type I), or with somewhat larger and more globular extensions (type II). Type III pits had a deeply invaginated surface with a smaller orifice than the other two types. In some cases, material could be seen inside these pits. The total density of pits in seawater-adapted tilapia gills decreased to 63 % of the density found in fresh water (Table 2). In fresh water, 63 % of all pits were type I. In seawater-adapted fish, only type III pits were found which were deep and had an orifice size similar to that of the freshwater type III pits (Fig. 4B; Table 2). In seawater-adapted fish, the density of type III pits was double that found in fresh water.

Comparison between fresh and fixed tissue

After fixation, the distance between 10 lamellae in the mid-region of the filament had decreased to 72.9 %, and the width of filaments to 75.6 %, of these dimensions in the same filaments before fixation (Table 3). This implies that the size of fixed cells was only 55 % of that of unfixed cells, which is a reduction of 46 % (assuming round cells and using πr^2 to

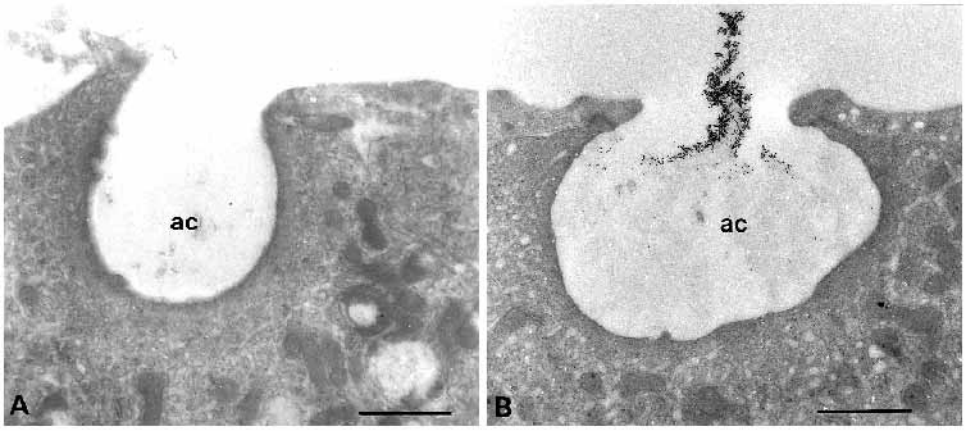

Fig. 3. Transmission electron micrographs of the apical crypt (ac) of a mature chloride cell from a freshwater-adapted tilapia labelled with (A) streptavidin-gold only (control) or (B) biotinylated Concanavalin-A followed by streptavidin-gold. When both labels were applied (B), large numbers of gold particles (diameter 10 nm) were found associated with glycoproteins in the apical crypts of chloride cells. Scale bar, 1 μm.

Table 1. *Density and size of mitochondria-rich (MR) cells (DASPMI-positive cells) and pits (Concanavalin-A–fluorescein conjugate binding areas; Con-A) in the top MR cell layer of non-fixed gill epithelium of freshwater- and seawater-adapted tilapia determined by confocal laser scanning microscopy*

	Fresh water	Sea water	Percentage change
Cell density (cells mm^{-2})			
DASPMI (total)	6233±713	3061±296*	51
Con-A	3419±534	2167±295*	37
DASPMI and Con-A	3458±553	2445±194*	29
Cell size (μm^2)			
DASPMI	87±9	217±69*	149

Values are means ± S.D. (*N*=4).

Cell size was determined as the maximum cross-sectional surface area of the cell.

*Significantly different from the freshwater group (P<0.05).

Table 2. *Density and size of pits in gill epithelium of freshwater- and seawater-adapted tilapia determined by scanning electron microscopy*

	Fresh water	Sea water	Percentage change
Pit density (pits mm^{-2})			
Type I	6924±637	none	–
Type II	773±991	none	–
Type III	3288±1523	6939±1163*	111
Total	10985	6939	37
Surface area of pits (μm^2)			
Type I	10.7±3.2	–	–
Type II	6.7±2.5	–	–
Type III	2.5±0.1	2.1±0.7	–

Values are means ± S.D. (*N*=3).

Type I pit: flat or shallow exposed surface with a network of small cellular extensions.

Type II pit: flat or shallow exposed surface with globular extensions.

Type III pit: deeply invaginated pit, occasionally filled with material of undefined origin.

*Significantly different from the freshwater group (P<0.05).

calculate the surface area, where r is cell radius). Figs 4 and 5 show micrographs of the epithelial surface made using SEM and CLSM, respectively. With CLSM, labelling of the microridges of pavement cells with Concanavalin-A–fluorescein conjugate could be visualized with a 60× objective only. The labelling was far less intense than for apical pits (see Fig. 5). The surface area of pavement cells decreased by 42.9 % after fixation (from 134±8.0 μm^2 to 76.5±16.4 μm^2, mean ± S.D.), a value in perfect agreement with the 46 % decrease anticipated (Table 3).

Na^+/K^+-ATPase activity

The total and specific Na^+/K^+-ATPase activities in gill homogenates were not significantly different (P>0.7, N=5) for seawater- and freshwater-adapted fish. The specific Na^+/K^+-ATPase activities (V_{spec}), determined as the amount of inorganic phosphates released, were (mean ± S.E.M.) 9.17±2.0 μmol P_i h^{-1} mg^{-1} in fresh water and 9.09±2.83 μmol P_i h^{-1} mg^{-1} in sea water. The total Na^+/K^+-ATPase activities were calculated as V_{spec}×mg protein and were 81.7±16.8 μmol P_i h^{-1} in fresh water and 89.6±13.6 μmol P_i h^{-1} in sea water.

Discussion

A new fluorescent double-labelling technique was used to differentiate between the total number of MR cells present in the unfixed gills of tilapia and the properties of those that were in contact with water. The findings were compared with results from biochemical measurements and standard microscopical techniques. The procedure is fast and allows qualitative and quantitative analyses.

CLSM using double-labelling of chloride cells

We used two fluorescent probes, DASPMI and Con-A–fluorescein conjugate, to identify MR cells that were in contact with the water. Specific vital dyes for mitochondria,

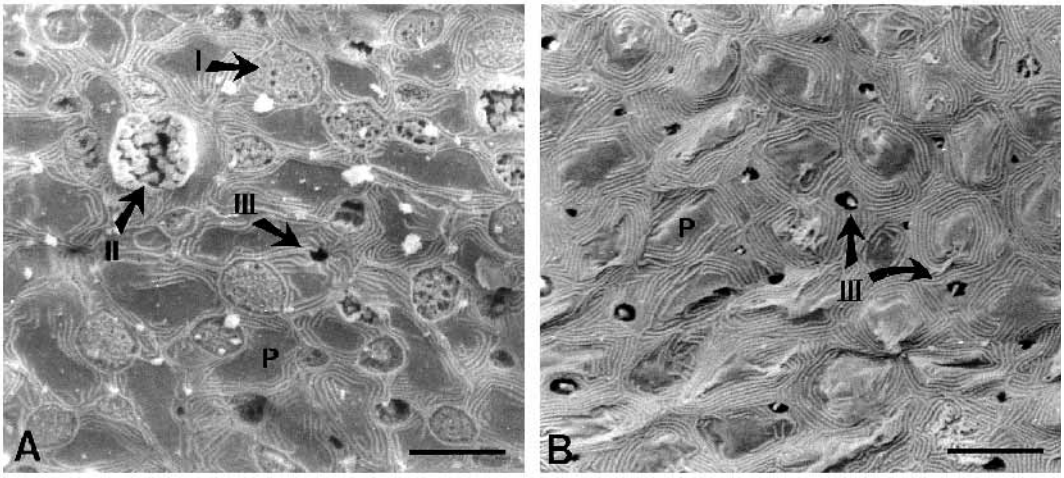

Fig. 4. Scanning electron micrograph of the trailing edge area from Fig. 1 of gills from (A) freshwater- and (B) seawater-adapted tilapia. P, pavement cell; I, type I pit with small cellular extensions; II, type II pit with globular extensions; III, type III pit with deeply invaginated exposed surface, occasionally with some material inside. Scale bar, 10 μm.

such as DASPEI and DASPMI, are suitable for identification and quantification of mitochondria-rich chloride cells in epithelia of teleosts (Bereiter-Hahn, 1976; Foskett and Scheffey, 1982; Karnaky *et al.* 1984; Marshall and Nishioka, 1980; McCormick *et al.* 1992). However, several groups have found morphologically different subtypes in the chloride cell population (Perry *et al.* 1992; Pisam *et al.* 1987; Wendelaar Bonga and van der Meij, 1989). Wendelaar Bonga and co-workers attribute differences in ultrastructure to the stage of the life cycle of the chloride cells. They distinguish accessory, immature, mature and degenerating (apoptotic and necrotic) cells. Of these subtypes, the mature chloride cells possess at least three features that could be attributed to a functional ion-transporting cell. First, they have many mitochondria, which may provide the energy required for active transepithelial ion transport against the large electrochemical gradients known to exist between the external medium and the blood (for a review see Evans, 1982). Second, they have an extensive network of tubules that are believed to be continuous with the basolateral membrane and where ion-transporting enzymes, such as Na^+/K^+-ATPase, Ca^{2+}-ATPase and Na^+/Ca^{2+} exchangers, are located (Karnaky *et al.* 1976; Flik *et al.* 1985*a*; Perry and Flik, 1988; Verbost *et al.* 1994). Third, they are in contact with both water (*via* the apical crypt) and blood (*via* the basolateral membrane). Since an abundance of mitochondria is found not only in mature, but also in accessory, immature and possibly in early degenerating chloride cells, it is likely that the use of DASPMI (and analogues) will label most subtypes and this will lead to an overestimation of the density of functional ion-transporting cells. We therefore used a second fluorescent label, fluorescein-conjugated Concanavalin-A, which specifically labels glycoproteins with α-mannopyranosyl and α-glucopyranosyl residues (Goldstein *et al.* 1969). It appeared that the contents and/or membrane surface of apical pits of chloride cells include a relatively higher level of such glycoproteins than the other cells present in this epithelium, since the lectin bound strongly to the apical surface of chloride cells (see Fig. 2 where the fluorescein-conjugated Con-A binds to DASPMI-positive cells, and Fig. 3 where streptavidin-gold

Table 3. *Comparison of the size of gill filaments and pavement cells of freshwater-adapted tilapia before and after fixation for scanning electron microscopy*

		Prefixation	Postfixation	Percentage shrinkage
Filaments	length[1] (μm)	454±15	331±10*	27.1
	width[1] (μm)	504±19	381±11*	24.4
Pavement cell	Surface area[2] (μm^2)	134±8.0	76.5±16.4*	42.9

Values are means ± S.D. (N=5).

[1]Distances were measured between 10 lamellae (length) and leading and trailing edge (width) at the mid-region of the filament.

[2]Measured using confocal laser scanning microscopy and Concanavalin-A–fluorescein conjugate in freshly isolated filaments and using scanning electron microscopy after fixation.

*Significantly different from the prefixation group (P<0.001).

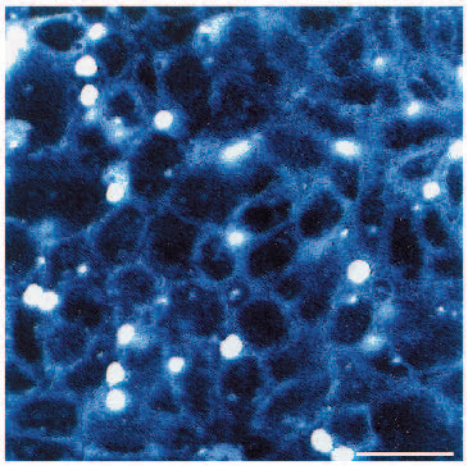

Fig. 5. Confocal laser scanning micrograph of the surface of freshwater-adapted gill filaments labelled with fluorescein-conjugated Concanavalin-A. The fluorescence intensity of the label is extremely strong in the apical pits (white) and less strong on the concentrically arranged microridges of pavement cells (coloured blue). Scale bar, 25 μm.

particles are concentrated in the apical crypt prelabelled with biotinylated Concanavalin-A). Different lectins have been used before in studies of intercalated cells, which are the MR cells in the mammalian kidney (Brown *et al.* 1985; Schuster *et al.* 1986). It was found that these cells could be divided into two subtypes (α and β) on the basis of different functions and binding capacity for the lectins. Our electron microscopical observations on lectin-labelled filaments do not suggest a similar heterogeneity in chloride cell lectin-binding capacity. Furthermore, a small number of gold particles was found on pavement cells (data not shown), indicating that these cells were also able to bind the lectin. This latter observation was not surprising since the fluorescein-labelled Concanavalin-A could also be visualized (using a high magnification) on pavement cells using CLSM (Fig. 5). The difference in lectin-binding capacity between the branchial epithelial cell types is in agreement with ultrastructural studies of the glycocalyx of gill cells showing that the thickness (Powell *et al.* 1994) and composition (Pisam *et al.* 1980) of the cell coat of chloride cells is different to that of pavement cells, mucocytes or adjacent cells. Thus, when both DASPMI and Concanavalin-A–fluorescein conjugate labels are present in/on the same cell, this is probably a mature (functional) chloride cell. The group of cells that are only labelled by DASPMI, may represent accessory, immature and degenerating chloride cells. The relative frequency of occurrence of these cells in freshwater fish (55 % of the DASPMI-positive cells) is in accordance with that found using TEM (Wendelaar Bonga *et al.* 1990), but we would need other labels with specificity for each cell subtype to confirm this. By using the two probes and serial scans in the *z*-direction, one can show the distribution pattern of MR cells across the filament and quantify the total and mature MR cell density and size in any layer of unfixed multilayered gill tissue. However, one has to keep in mind that the measurement of the perimeter of DASPMI-positive cells only gives an approximation of the real chloride cell size, as the cell membrane itself is not labelled. Furthermore, a restriction applies to the use of Concanavalin-A for determination of the exact size or volume of the apical pit as we do not know to what extent the glycoprotein composition and content in the apical crypt change in differently adapted fish and how this influences the degree of Con-A binding.

In these studies with unfixed tissue, one has to beware of structural changes that may occur in the epithelium during the time of preparation which, to the moment of scanning, could be 1 h. For species such as striped bass *Morone saxatilis*, which can stand abrupt changes in salinity, a time span of 3 h is long enough to induce changes in the exposed area of the apical surface of chloride cells in living fish (King and Hossler, 1991). However, Mozambique tilapia seem to adapt more slowly: on transfer from fresh water to sea water, no ultrastructural changes are induced within the first few hours (Hwang, 1987). This observation also applies to filaments when they are kept in an incubation medium *in vitro*, as shown by our finding that there was no difference in the measured mature chloride cell density after *in vitro* (as used in this study) or *in vivo* labelling of tilapia gills (Li *et al.* 1995). In the latter case, the gills were labelled by allowing the fish to swim in the vital stain dissolved in water, and only 5 min passed between excision of the gills and examination. This finding suggests that data from our study reflect the *in vivo* situation.

SEM of gill filaments

In this study on tilapia, we were unable to discriminate in all cases between a mucus cell and a chloride cell on the basis of the external appearance of the apical surface of these cells. In previous SEM studies, the exposed apical surface of chloride cells has been used to identify and quantify mature chloride cells (Hossler *et al.* 1985; King and Hossler, 1991; Perry *et al.* 1992). From TEM and light microscope studies, it is known that both chloride cells and mucocytes are present on the trailing edge of tilapia filaments (on the area indicated in Fig. 1) in different salinities and that the density of mucocytes decreases in sea water (Wendelaar Bonga and van der Meij, 1989; Cioni *et al.* 1991). These TEM studies on tilapia also showed that the apical surface of chloride cells in freshwater-adapted fish is folded into small projections and is either flat (like type I in Fig. 4A) or forms an apical cavity (like the type III pit). Because of the presence of globular structures in or on the type II pits, these pits most resembled the apical pores of mucocytes with mucosomes. However, with a deep apical cavity, a chloride cell cannot be discriminated from a mucus cell and, therefore, the type III pits could belong to either cell type. In some cases, material could be seen inside these pits, but it was impossible to tell whether this was secreted mucus or the folded apical membrane. Chloride cells are probably represented by type I pits and an (unknown) proportion of type III pits. In TEM pictures from seawater-adapted fish, the apical cavities appear to be deeper, and in our SEM study only type III pits were found. Because mucocytes are also known to be present on the gill filament trailing edge in seawater fish, type III pits in seawater fish will certainly include the apical pores of mucocytes. The possibility that mucocytes are present among the type III pits may lead to an overestimation of the numbers of this type of pit. A further complicating factor in the estimation of mature chloride cell density is the presence of multicellular complexes, which were present in both freshwater- and seawater-adapted tilapia, although with a much higher frequency in seawater fish. Thus, an estimate of mature chloride cells based on the number of pits in SEM pictures will lead to a small underestimation in freshwater gills and a large underestimation in seawater gills. Taken together, we conclude that SEM analysis does not allow an accurate estimation of mature chloride cell density in tilapia gill filaments on the basis of the number of apical pits.

There is a large discrepancy between the density of ‘mature’ chloride cells found using CLSM (represented by the density of doubly labelled cells) and SEM (type I and a portion of type III pits). If all type III pits were apical crypts of chloride cells, then numbers estimated from SEM would be higher by a factor of 3 than numbers from CLSM, both in freshwater- and seawater-adapted fish. To a large extent, this can be explained

by shrinkage of the tissue after fixation. Both at the cellular level (size of pavement cells) and the level of the whole filament, a decrease in length and width of approximately 25 % was observed. However, even after correction for shrinkage, the density of pits in seawater gills found using SEM exceeds the total density of chloride cells found using CLSM. The advantage of CLSM analysis using double labelling, is that pits in DASPMI-positive cells can be designated as apical crypts, whereas pits observed by SEM cannot be definitely identified as apical pits or mucus cell pits. The discrepancy between the numbers observed using CLSM and with SEM remains unexplained: it may be caused by the drying method used for the SEM. Changes in size during fixation should be minimal since osmolarity of the fixative was similar to the osmolarity of the blood of the fish. Another aspect of this SEM analysis concerns the orifice size of the pits which was smaller in sea water than in fresh water. Because of the folded nature of the apical membrane (and folding appears even more elaborate in sea water), it cannot be concluded that the actual apical surface on the chloride cell also decreases.

Effect of salinity

In freshwater fish, the gills are the site of active ion absorption for growth and homeostasis, and this uptake compensates for losses through branchial diffusion and urinary excretion. In seawater fish, Na^+ and Cl^- are absorbed through the gills, skin and intestine and the surplus is excreted *via* the gills. Physiological and electrophysiological data favour the thesis that Ca^{2+} is actively absorbed by the gills in fresh water as well as in sea water (McCormick *et al.* 1992; Verbost *et al.* 1994; Marshall *et al.* 1995; Flik *et al.* 1996). Euryhaline fishes, such as the Mozambique tilapia, can adapt to different salinities and thus must be able to reverse branchial Na^+ and Cl^- fluxes completely. Assuming that active transport of these ions across the gills occurs exclusively through functional chloride cells, one can predict regulation at the level of these cells: density, spatial distribution and permeability between junctions of chloride cells, size of apical exposure area and enzymatic composition may change according to the ambient medium. The character of the changes depends on multiple factors that determine the electrochemical condition of the epithelium, such as ion displacement and diffusion of water as a result of the ion composition of the medium and plasma. Another complicating factor is the multifunctionality of the gills, since they are involved not only in osmoregulation but also in respiratory gas exchange, excretion of nitrogenous waste products and acid–base regulation, processes that are all intimately linked.

We found no differences in Na^+/K^+-ATPase activity of gill homogenates between freshwater- and seawater-adapted tilapia, which is in agreement with some previous reports (Kültz and Jürss, 1991; Verbost *et al.* 1994). Others have found an increase in Na^+/K^+-ATPase activity following seawater adaptation in this species (Dharmamba *et al.* 1975; Dange, 1985; Young *et al.* 1988; Kültz *et al.* 1992), which is in agreement with the general picture for euryhaline species (Borgatti *et al.* 1992). The finding that the total Na^+/K^+-ATPase activity was unchanged, while the total number of MR cells decreased in sea water, suggests that the amount of Na^+/K^+-ATPase per cell had increased. This is consistent with the increased size of the cells in sea water, which is accompanied by expansion of the tubular system in those cells where the branchial Na^+/K^+-ATPase is located (Karnaky *et al.* 1976; Hootman and Philpott, 1979). However, these data refer to the total capacities rather than the operational activities of the enzymes in the tissue. Moreover, these data are based on total chloride cell populations.

Our SEM observations do not allow us to draw any conclusion on how the density of mature chloride cells changes with salinity. However, our data do show that the apical pits of chloride cells (and perhaps also mucus cells) of tilapia change morphology in response to a salinity change. It is tempting to state that this change is related to a change in ion transport.

Quantification of the total number of MR cells in the top chloride cell layer (the true top layer of the epithelium consists of pavement cells covering the chloride cells) of the trailing edge shows that there was a 51 % decrease in density after seawater adaptation compared with freshwater levels. At the same time, the size of these cells increased by 149 %. When these figures are combined, the relative ‘occupation’ of MR cells in the top layer of the filament can be calculated by multiplying total MR cell density by cell size and dividing this by the surface area. It then appears that the space occupied by MR cells increases from 54 to 66 %. When the density of active chloride cells, defined as those chloride cells with their apical membrane (pit) exposed to the water, was quantified, a 29 % decrease after seawater adaptation was found.

Taking these results together, we conclude that regulation of the ion-transporting capacity of the gills of tilapia adapted to different salinities involves a replacement of ion-transporting cells with cells that differ in morphology and number. Previous TEM observations on the same species under similar conditions (Wendelaar Bonga and van der Meij, 1989) led us, on the basis of the increased frequency of apoptotic and immature cells, to conclude that the turnover rate of chloride cells in sea water compared with that in fresh water had increased.

Perspectives

In future studies, we will focus on the further characterization of the MR cell population in the branchial epithelium. We are currently evaluating procedures that will combine mitochondrial vital stains with the terminal deoxynucleotidyl-transferase-mediated biotinylated deoxyuridine triphosphate nick end labeling (TUNEL) procedure for apoptosis (Sgonc *et al.* 1994). This combination of labelling may allow us to gain a better insight into chloride cell turnover under various stressful conditions.

We wish to thank Mr J. C. A. van der Meij for carrying out the TEM studies. The research of A.J.H.v.d.H. was subsidised

by the Netherlands Foundation for Life Sciences (SLW) of the Netherlands Organization for Scientific Research (NWO).

References

BEREITER-HAHN, J. (1976). Dimethylaminostyrylmethylpyridinium-iodine (DASPMI) as a fluorescent probe for mitochondria *in situ*. *Biochim. biophys. Acta* **423**, 1–14.

BERRIDGE, M. J. AND OSCHMAN, J. L. (1972). *Transporting Epithelia*. New York, London: Academic Press.

BORGATTI, A. R., PAGLIARANI, A. AND VENTRELLA, V. (1992). Gill Na^+/K^+-ATPase involvement and regulation during salmonid adaptation to salt water. *Comp. Biochem. Physiol* A **102**, 637–643.

BROWN, D., ROTH, J. AND ORCI, L. (1985). Lectin-gold cytochemistry reveals intercalated cell heterogeneity along rat kidney collecting ducts. *Am. J. Physiol.* **248**, C328–C356.

CIONI, C., DE MERICH, D., CATALDI, E. AND CATAUDELLA, S. (1991). Fine structure of chloride cells in freshwater- and seawater-adapted *Oreochromis niloticus* (Linnaeus) and *Oreochromis mossambicus* (Peters). *J. Fish Biol.* **39**, 197–209.

DANGE, A. D. (1985). Branchial Na^+/K^+-ATPase activity during osmotic adjustments in two freshwater euryhaline teleosts, tilapia (*Sarotherodon mossambicus*) and orange chromid (*Etroplus maculatus*). *Mar. Biol.* **87**, 101–107.

DE RENZIS, G. AND BORNANCIN, M. (1984). Ion transport and gill ATPases. In *Fish Physiology*, vol. 10 (ed. W. S. Hoar and D. J. Randall), pp. 65–104. London: Academic Press.

DHARMAMBA, M., BORNANCIN, M. AND MAETZ, J. (1975). Environmental salinity and sodium and chloride exchanges across the gill of *Tilapia mossambica*. *J. Physiol., Lond.* **70**, 627–636.

EVANS, D. H. (1982). Salt and water exchange across vertebrate gills. In *Gills* (ed. D. F. Houlihan and T. J. Shuttleworth). *Society of Experimental Biology Seminar Series* **16**, 149–171. Cambridge: Cambridge University Press.

FLIK, G., KLAREN, P. H. M., SCHOENMAKERS TH., J. M., BIJVELDS, M. J. C., VERBOST, P. M. AND WENDELAAR BONGA, S. E. (1996). Cellular calcium transport in fish: unique and universal mechanisms. *Physiol. Zool.* **69**, 403–417.

FLIK, G., RIJS, J. H. AND WENDELAAR BONGA, S. E. (1985*a*). Evidence for high-affinity Ca^{2+}-ATPase activity and ATP-driven Ca^{2+}-transport in membrane preparations of the gill epithelium of the cichlid fish *Oreochromis mossambicus*. *J. exp. Biol.* **119**, 335–347.

FLIK, G. AND VERBOST, P. M. (1993). Calcium transport in fish gills and intestine. *J. exp. Biol.* **184**, 17–29.

FLIK, G., VERBOST, P. M. AND WENDELAAR BONGA, S. E. (1995). Calcium transport processes in fishes. In *Fish Physiology*, vol. 14 (ed. W. S. Hoar, D. J. Randall and A. P. Farrell), pp. 317–342. San Diego: Academic Press, Inc.

FLIK, G., WENDELAAR-BONGA, S. E. AND FENWICK, J. C. (1983). Ca^{2+}-dependent phosphatase and ATPase activities in eel gill plasma membranes. I. Identification of Ca^{2+}-activated ATPase activities with non-specific phosphatase activities. *Comp. Biochem. Physiol.* B **76**, 745–754.

FLIK, G., WENDELAAR-BONGA, S. E. AND FENWICK, J. C. (1985*b*). Active Ca^{2+} transport in plasma membranes of branchial epithelium of the North-American eel, *Anguilla rostrata* LeSueur. *Biol. Cell* **55**, 265–272.

FOSKETT, J. K. AND SCHEFFEY, C. (1982). The chloride cell: definitive identification as the salt-secretory cell in teleosts. *Science* **215**, 164–166.

GOLDSTEIN, I. J., SO, L. L., YOUNG, Y. AND COLLIES, Q. C. (1969). Protein carbohydrate interaction. XIX. The interaction of Concanavalin A with IgM and the glycoprotein phytoagglutinins of the waxbean and soybean. *J. Immun.* **103**, 695–698.

HOOTMAN, S. R. AND PHILPOTT, C. W. (1979). Ultracytochemical localization of Na^+,K^+-activated ATPase in chloride cells from the gills of a euryhaline teleost. *Anat. Rec.* **193**, 99–129.

HOSSLER, F. E., MUSIL, G., KARNAKY, K. J. AND EPSTEIN, F. H. (1985). Surface ultrastructure of the gill arch of the killifish, *Fundulus heteroclitus*, from seawater and fresh water, with special reference to the morphology of apical crypts of chloride cells. *J. Morph.* **185**, 377–386.

HWANG, P. P. (1987). Tolerance and ultrastructural responses of branchial chloride cells to salinity changes in the euryhaline teleost *Oreochromis mossambicus*. *Mar. Biol.* **94**, 643–649.

KARNAKY, K. J., JR, DEGNAN, K. J., GARRETSON, L. T. AND ZADUNAISKY, J. A. (1984). Identification and quantification of mitochondria-rich cells in transporting epithelia. *Am. J. Physiol.* **246**, R770–R775.

KARNAKY, K. J., JR, KINTER, L. B., KINTER, W. B. AND STIRLING, C. E. (1976). Teleost chloride cell. II. Autoradiographic localization of gill Na,K-ATPase in killifish *Fundulus heteroclitus* adapted to low and high salinity environments. *J. Cell Biol.* **70**, 157–177.

KING, J. A. C. AND HOSSLER, F. E. (1991). The gill arch of the striped bass (*Morone saxatilis*). IV. Alterations in the ultrastructure of chloride cell apical crypts and chloride efflux following exposure to seawater. *J. Morph.* **209**, 165–176.

KÜLTZ, D. AND JÜRSS, K. (1991). Acclimation of chloride cells and Na^+/K^+-ATPase to energy deficiency in tilapia (*Oreochromis mossambicus*). *Zool. Jb. Physiol.* **95**, 39–50.

KÜLTZ, D., BASTROP, R., JÜRSS, K. AND SIEBERS, D. (1992). Mitochondria-rich (MR) cells and the activities of the Na^+/K^+-ATPase and carbonic anhydrase in the gill and opercular epithelium of *Oreochromis mossambicus* adapted to various salinities. *Comp. Biochem. Physiol.* B **102**, 293–301.

LI, J., EYGENSTEYN, J., LOCK, R. A. C., VERBOST, P. M., VAN DER HEIJDEN, A. J. H., WENDELAAR BONGA, S. E. AND FLIK, G. (1995). Branchial chloride cells in larvae and juveniles of freshwater tilapia *Oreochromis mossambicus*. *J. exp. Biol.* **198**, 2177–2184.

MARSHALL, W. S., BRYSON, S. E., BURGHARDT, J. S. AND VERBOST, P. M. (1995). Ca^{2+} transport by opercular epithelium of the freshwater-adapted euryhaline teleost, *Fundulus heteroclitus*. *J. comp. Physiol.* B **165**, 268–277.

MARSHALL, W. S. AND NISHIOKA, R. S. (1980). Relation of mitochondria-rich chloride cells to active chloride transport in the skin of a marine teleost. *J. exp. Zool.* **214**, 147–156.

MCCORMICK, S. D., HASEGAWA, S. AND HIRANO, T. (1992). Calcium uptake in the skin of a freshwater teleost. *Proc. natn. Acad. Sci. U.S.A.* **89**, 3635–3638.

PERRY, S. F. AND FLIK, G. (1988). Characterization of branchial transepithelial calcium fluxes in freshwater trout, *Salmo gairdneri*. *Am. J. Physiol.* **254**, R491–R498.

PERRY, S. F., GOSS, G. G. AND LAURENT, P. (1992). The interrelationships between gill chloride cell morphology and ionic uptake in four freshwater teleosts. *Can. J. Zool.* **70**, 1775–1786.

PERRY, S. F. AND RANDALL, D. J. (1981). Effects of amiloride and SITS on branchial ion fluxes in rainbow trout, *Salmo gairdneri*. *J. exp. Zool.* **215**, 225–228.

PISAM, M., CAROFF, A. AND RAMBOURG, A. (1987). Two types of chloride cells in the gill epithelium of a freshwater-adapted

euryhaline fish: *Lebistes reticularis*; their modifications during adaptation to seawater. *Am. J. Anat*. **179**, 40–50.

PISAM, M. AND RAMBOURG, A. (1991). Mitochondria-rich cells in the gill epithelium of teleost fishes: an ultrastructural approach. *Int. Rev. Cytol.* **130**, 191–232.

PISAM, M., SARDET, C. AND MAETZ, J. (1980). Polysaccharidic material in chloride cell of teleostean gill: modifications according to salinity. *Am. J. Physiol.* **238**, R213–R218.

POWELL, M. D., SPEARE, D. J. AND WRIGHT, G. M. (1994). Comparative ultrastructural morphology of lamellar epithelial, chloride and mucus cell glycocalyx of the rainbow trout (*Oncorhynchus mykiss*) gill. *J. Fish Biol.* **44**, 725–730.

PRATAP, H. B. AND WENDELAAR BONGA, S. E. (1993). Effect of ambient and dietary cadmium on pavement cells, chloride cells and Na^+/K^+-ATPase activity in the gills of the freshwater teleost *Oreochromis mossambicus* at normal and high calcium levels in the ambient water. *Aquat. Toxicol.* **26**, 133–150.

SCHUSTER, V. L., BONSIB, S. M. AND JENNINGS, M. L. (1986). Two types of collecting duct mitochondria-rich (intercalated) cells: lectin and band 3 cytochemistry. *Am. J. Physiol.* **251**, C347–C355.

SGONC, R., BOECK, G., DIETRICH, H., GRUBER, J., RECHEIS, H. AND WICK, G. (1994). Simultaneous determination of cell surface antigens and apoptosis. *Trends Genet.* **10**, 41–42.

SMITH, H. W. (1930). The absorption and excretion of water and salts by marine teleosts. *Am. J. Physiol.* **93**, 480–505.

VERBOST, P. M., SCHOENMAKERS, T. J. M., FLIK, G. AND WENDELAAR BONGA, S. E. (1994). Kinetics of ATP- and Na^+-gradient driven Ca^{2+} transport in basolateral membranes from gills of freshwater- and seawater-adapted tilapia. *J. exp. Biol.* **186**, 95–108.

WENDELAAR BONGA, S. E., FLIK, G., BALM, P. H. M. AND VAN DER MEIJ, J. C. A. (1990). The ultrastructure of chloride cells in the gills of the teleost *Oreochromis mossambicus* during exposure to acidified water. *Cell Tissue Res.* **259**, 575–585.

WENDELAAR BONGA, S. E. AND VAN DER MEIJ, J. C. A. (1989). Degeneration and death, by apoptosis and necrosis, of the pavement and chloride cells in the gills of the teleost *Oreochromis mossambicus*. *Cell Tissue Res.* **255**, 235–243.

YOUNG, P. S., MCCORMICK, S. D., DEMAREST, J. R., LIN, R. J., NISHIOKA, R. S. AND BERN, H. A. (1988). Effects of salinity, hypophysectomy and prolactin on whole-animal transepithelial potential in the tilapia *Oreochromis mossambicus*. *Gen. comp. Endocr.* **71**, 389–397.

ZADUNAISKY, J. A., CARDONA, S., AU, L., ROBERTS, D. M., FISHER, E., LOWENSTEIN, B., CRAGOE, E. J. AND SPRING, K. R. (1995). Chloride transport activation by plasma osmolarity during rapid adaptation to high salinity of *Fundulus heteroclitus*. *J. Membr. Biol.* **143**, 207–217.